Table VII. Complete Assignment of Normal Modes to C_{4v} Symmetry Notations and Atomic Group Vibrations

	symm	arguments from	H	D	assignt
ν_1	a_1	R	480	440	σ(Cr-NH_3)
ν_2	a_1	IR	438	413	
ν_3	b_1	R	448	416	
ν_4	e	IR	463	432	
ν_5	a_1	far-IR	342	333	σ(Cr-NCO)
ν_6	a_1	abs	281	235	δ(H_3N-Cr-NH_3)
ν_7	b_1	far-IR	158	148	
ν_8	b_2	far-IR	236	214	
ν_9	e	far-IR	220	204	
ν_{10}	e	abs	255	235	
ν_{11}	e	far-IR	177	172	δ(H_3N-Cr-NCO)
ν_{16}	e	abs	645	512	δ(Cr-N-H)
ν_{17}	e	abs	685	540	
ν_{18}	e	IR + abs	760	600	
ν_{19}	e	far-IR	195	195	δ(Cr-N-C) (?)
ν_{20}	e	IR	605	609	δ(N-C-O)
ν_{21}	a_1	IR	1315	1292	σ(NC-O)
ν_{22}	a_1	IR	2240	2220	σ(N-CO)

compared to the ground state. From infrared, Raman, and vibronic data in absorption and emission, it is certain that the ν_5 frequency in the excited electronic states is greater than in the ground state, with a frequency factor[17] of $\beta = 351/342 = 1.02$ if, e.g., the vibronic $^2A_1$ sideband of the undeuterated compound (cf. see Tables II, III, and VI) is considered. This is quite unusual: generally, the potential curves of excited states indicate force constants which are lower than those in the ground state.[2,7] The steeper potential curve in the excited state may be explained by coupling of a large number of electronic states by virtue of the low symmetry.

Conclusions

In Table VII the results obtained from the above discussion on symmetry assignments to band peaks, using different spectroscopic techniques, are compiled. The assignment to vibrations of atomic groups as derived from symmetry vibrations (see Table I) is also included. While most of these assignments appear certain, some others are still tentative. Further investigations with other techniques or a complete normal-coordinate analysis must be carried out if more definite assignments are to be made. The other main concern of this paper is the determination of the order of doublet energy level splittings resulting from the low-symmetry, in order to come to a decision on the inconsistencies in the literature. All results support the view that convential ligand field theory is unable to explain the large low-symmetry effects on energy levels of low multiplicity found experimentally.

Acknowledgment. The authors are indebted to the Ministerium für Wissenschaft und Forschung des Landes Nordrhein-Westfalen, Düsseldorf, and the Verband der Chemischen Industrie, Frankfurt, for financial support. We also thank Mr. Rolf Linder, Düsseldorf, for his technical assistance in the construction of some spectroscopic devices.

Registry No. $[Cr(NH_3)_5(NCO)](NO_3)_2$, 68092-88-6.

References and Notes

(1) A. M. Black and C. D. Flint, *J. Chem. Soc., Faraday Trans. 2*, **73**, 877 (1977).
(2) R. Wernicke and H.-H. Schmidtke, *Mol. Phys.*, **37**, 607 (1979).
(3) S. M. Khan, H. H. Patterson, and H. Engstrom, *Mol. Phys.*, **35**, 1623 (1978).
(4) R. Wernicke, G. Eyring, and H.-H. Schmidtke, *Chem. Phys. Lett.*, **58**, 267 (1978).
(5) S. L. Chodos, A. M. Black, and C. D. Flint, *J. Chem. Phys.*, **65**, 4816 (1976).
(6) C. D. Flint and A. P. Matthews, *J. Chem. Soc., Faraday Trans. 2*, **70**, 1301 (1974).
(7) C. D. Flint and A. P. Matthews, *J. Chem. Soc., Faraday Trans. 2*, **69**, 419 (1973).
(8) W. N. Shephard and L. S. Forster, *Theor. Chim. Acta*, **20**, 135 (1971).
(9) S. Decurtins, H. U. Güdel, and K. Neuenschwander, *Inorg. Chem.*, **16**, 796 (1977).
(10) H.-H. Schmidtke and T. Schönherr, *Z. Anorg. Allg. Chem.*, **443**, 225 (1978).
(11) J. R. Perumareddi, *Coord. Chem. Rev.*, **4**, 73 (1969).
(12) N. Tanaka, M. Kamada, J. Fujita, and E. Kyuno, *Bull. Chem. Soc. Jpn.*, **37**, 222 (1964).
(13) K. H. Schmidt and A. Müller, *J. Mol. Struct.*, **22**, 343 (1974).
(14) M. W. Bee, S. F. A. Kettle, and D. B. Powell, *Spectrochim. Acta, Part A*, **30a**, 139 (1974).
(15) P. E. Hoggard, T. Schönherr, and H.-H. Schmidtke, *Spectrochim. Acta, Part A*, **32a**, 917 (1976).
(16) H. Homborg and W. Preetz, *Spectrochim. Acta, Part A*, **32a**, 709 (1976).
(17) H. Kupka, *Mol. Phys.*, **36**, 685 (1978).
(18) C. D. Flint, A. P. Matthews, and P. J. O'Grady, *J. Chem. Soc., Faraday Trans. 2*, **73**, 655 (1977).
(19) R. M. MacFarlane, *J. Chem. Phys.*, **47**, 2066 (1967).

Contribution from the Institut für Anorganische Chemie, Universität Bern, CH-3000 Bern 9, Switzerland, and the Institut für Reaktortechnik ETHZ, CH-5303 Würenlingen, Switzerland

Electronic Ground-State Properties of Tetranuclear Hexa-μ-hydroxo-bis(tetraamminechromium(III))bis(diamminechromium(III)) Chloride. A Spectroscopic and Magnetochemical Study

HANS U. GÜDEL,* URS HAUSER, and ALBERT FURRER

Received March 20, 1979

Magnetic susceptibility, optical spectroscopic, and inelastic neutron-scattering experiments were performed in order to investigate the exchange coupling in deuterated rhodoso chloride, $[Cr_4(OD)_6(ND_3)_{12}]Cl_6 \cdot 4D_2O$. Optical spectra illustrate the splitting of both ground and excited electronic states. By use of neutron inelastic scattering, transitions within the exchange split ground state were measured. Five inelastic peaks were resolved and analyzed in terms of an isotropic exchange Hamiltonian containing three bilinear and two biquadratic coupling parameters. The magnetic susceptibility curve does not contain enough structure to allow the determination of five exchange parameters by a least-squares fit.

Introduction

The tetranuclear rhodoso complex, hexa-μ-hydroxo-bis(tetraamminechromium(III))bis(diamminechromium(III)), first described by Jørgensen[1] almost 100 years ago, has a planar structure with the Cr^{3+} ions forming a regular rhombus (Figure 1).[2] Its structure is closely related to the Pfeiffer cation, $[Cr_4(OH)_6(en)_6]^{6+}$,[3] the magnetic properties of which have been studied in detail.[4-6] No magnetochemical investigation of the rhodoso complex has been reported.

Rather conflicting results have been obtained for the Pfeiffer ion. On the basis of the magnetic susceptibility measurements of the azide, Flood et al.[4] found both J and J' to be antiferromagnetic with a J/J' ratio of 0.53. Iwashita et al.,[5] on

* To whom correspondence should be addressed at the Institut für Anorganische Chemie, Universität Bern.

0020-1669/79/1318-2730$01.00/0

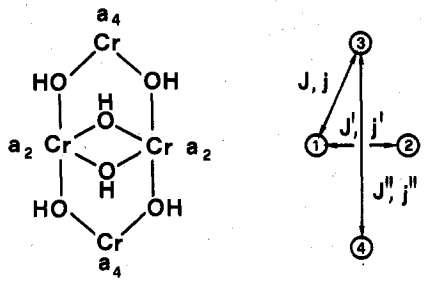

Figure 1. Schematic structure of the rhodoso complex $[Cr_4(OH)_6(NH_3)_{12}]^{6+}$, on the left-hand side. Exchange interaction parameters are defined on the right-hand side.

the other hand, on the basis of the same measurements, postulated a very large ferromagnetic coupling between Cr_1 and Cr_2. They also found it necessary to include higher order spin-coupling terms in their effective Hamiltonian. Sorai and Seki,[6] in their heat capacity study of Pfeiffer sulfate, derived antiferromagnetic exchange parameters J and J' as well as a rather large antiferromagnetic J''.

The magnetic properties of Na_3RuO_4 have recently been interpreted in terms of a cluster model which is closely related to the rhodoso and Pfeiffer ions.[7] However, a Schottky-type anomaly in the heat capacity curve expected for this model has not been observed experimentally.

In the present study magnetochemical techniques were combined with spectroscopic methods to study the effects of exchange interactions in deuterated rhodoso chloride. Neutron inelastic scattering proved to be the most valuable spectroscopic technique, since it allows the direct observation of exchange splittings in the ground state.

Experimental Section

Since a deuterated sample is required for the neutron scattering experiments and since preliminary magnetic susceptibility measurements revealed a very slight difference between deuterated and undeuterated forms at low temperatures, all the physical measurements reported here were performed on samples which were approximately 90% deuterated.

Preparation. $[Cr_4(OH)_6(NH_3)_{12}]Cl_6 \cdot 4H_2O$ was prepared according to Bang,[2] a procedure which follows the original preparation by Jørgensen.[1] The compound was found to crystallize in two different modifications depending on the speed of crystallization. The modification used for our measurements is identical with that used by Bang for the crystal structure determination. It is obtained on slow crystallization.

$[Cr_4(OD)_6(ND_3)_{12}]Cl_6 \cdot 4D_2O$ was obtained as follows. A saturated solution of rhodoso chloride in D_2O at 7 °C is left in the refrigerator for 14 h. The product is then precipitated by very slow addition of solid NaCl, cooling in a ice/NaCl/water mixture, and quick filtration. This procedure is repeated three times, yielding a product which is 90% deuterated. X-ray powder patterns of deuterated and undeuterated forms are identical.

Magnetic Susceptibility. Powder susceptibility measurements were done at the Laboratorium für Festkörperphysik, ETH, Zürich. A moving-sample technique was used, details of which have been described elsewhere.[8] The temperature was measured with a chromel/gold–iron thermocouple. The estimated accuracy of the temperature measurement is ±0.2 K. The magnetic field employed was 1 T. No field dependence was found for fields smaller than 2 T. For the fits of theoretical models to the susceptibility standard least-squares procedures were used. The weighting function was based on the estimated standard deviation of a single measurement.

Optical Spectroscopy. Absorption measurements were done on single crystals by using a Cary 17 spectrometer. Light was propagating perpendicular to the well-developed (101) faces of the monoclinic crystal. The light was polarized by a pair of Glan-Taylor prisms. Cooling was achieved by a helium gas-flow technique.

For the excitation of luminescence spectra the light of a 150-W sealed-beam Xe lamp was dispersed by a Spex Minimate monochromator. The luminescence was dispersed by a $^3/_4$ m Spex monochromator and detected by a cooled RCA 31034 PMT using both dc and photon counting techniques.

Neutron Inelastic Scattering. The principle of this technique as applied to exchange-coupled polynuclear complexes has been described elsewhere.[9,10] Measurements were done at the reactors Diorit and Saphir in Würenlingen. Both classical triple-axis and multiangle reflecting crystal (MARC) spectrometers were used. Incident neutron energies for the various experiments were chosen in the range 35–240 cm^{-1}, depending on the objective of the experiment. The experiments were done on a polycrystalline sample sealed in an aluminum cylinder of 1.5-cm diameter and 5-cm length.

All the experiments reported here were done in the energy-loss configuration, i.e., energy being transferred from the neutron beam to the molecular system during the scattering process.

Exchange Interactions

The point group symmetry of the tetranuclear cation in rhodoso chloride is C_i. However, within the experimental accuracy of the X-ray crystal structure determination the Cr^{3+} ions form a regular rhombus and all the Cr–O–Cr angles of the monohydroxo bridges are the same.[2] The approximate point symmetry is therefore D_{2h}. Within this approximation all four interactions along the edges of the rhombus are the same.

There is no experimental evidence for intermolecular interactions in the temperature range we are interested in. For the intramolecular coupling we adopt the scheme shown in (1)

$$\vec{S}_{12} = \vec{S}_1 + \vec{S}_2 \qquad \vec{S}_{34} = \vec{S}_3 + \vec{S}_4 \qquad \vec{S} = \vec{S}_{12} + \vec{S}_{34} \quad (1)$$

(cf. Figure 1). The wave functions of the coupled system are then of the form

$$|(S_1,S_2)S_{12}(S_3,S_4)S_{34}SM\rangle$$

or simply

$$|S_{12}S_{34}SM\rangle \quad (2)$$

Since $S_1 = S_2 = S_3 = S_4 = {}^3/_2$, both S_{12} and S_{34} can take the values 0, 1, 2, or 3 and $|S_{12} - S_{34}| \leq S \leq S_{12} + S_{34}$. For the description of the energy splitting we use an empirical Heisenberg-type Hamiltonian

$$\hat{H}_{ex} = J(\vec{S}_1\cdot\vec{S}_3 + \vec{S}_1\cdot\vec{S}_4 + \vec{S}_2\cdot\vec{S}_3 + \vec{S}_2\cdot\vec{S}_4) + J'\vec{S}_1\cdot\vec{S}_2 + J''\vec{S}_3\cdot\vec{S}_4 - j\{(\vec{S}_1\cdot\vec{S}_3)^2 + (\vec{S}_1\cdot\vec{S}_4)^2 + (\vec{S}_2\cdot\vec{S}_3)^2 + (\vec{S}_2\cdot\vec{S}_4)^2\} - j'(\vec{S}_1\cdot\vec{S}_2)^2 - j''(\vec{S}_3\cdot\vec{S}_4)^2 \quad (3)$$

For the definition of the exchange parameters we refer to Figure 1. The first line in eq 3 contains only bilinear terms. In the course of our work (vide infra) we found it necessary to include biquadratic terms (second and third line in eq 3) to describe the observed splitting pattern.

The matrix of (3) is not diagonal in the basis (2). Griffith has outlined an elegant procedure, based on tensor operators, to evaluate matrix elements of an operator of type (3).[11] Following this procedure we obtain expression 4 for a general matrix element.

$$\begin{aligned}\langle S_{12}S_{34}S|\hat{H}_{ex}|S'_{12}S'_{34}S\rangle &= \delta(S_{12}S'_{12})\delta(S_{34}S'_{34})(-1)^{S_{12}+1}\times \\ &\Big[(15J' + {}^{15}/_2 j')\begin{Bmatrix} {}^3/_2 & {}^3/_2 & 1 \\ {}^3/_2 & {}^3/_2 & S_{12}\end{Bmatrix} - 30j'\times \\ &\begin{Bmatrix} {}^3/_2 & {}^3/_2 & 2 \\ {}^3/_2 & {}^3/_2 & S_{12}\end{Bmatrix}\Big] + \delta(S_{12}S'_{12})\delta(S_{34}S'_{34})(-1)^{S_{34}+1}\times \\ &\Big[(15J'' + {}^{15}/_2 j'')\begin{Bmatrix} {}^3/_2 & {}^3/_2 & 1 \\ {}^3/_2 & {}^3/_2 & S_{34}\end{Bmatrix} - 30j''\begin{Bmatrix} {}^3/_2 & {}^3/_2 & 2 \\ {}^3/_2 & {}^3/_2 & S_{34}\end{Bmatrix}\Big] + \\ &[(2S_{12}+1)(2S'_{12}+1)(2S_{34}+1)(2S'_{34}+1)]^{1/2}\times \\ &[(-1)^S + (-1)^{S_{12}+S'_{12}+S} + (-1)^{S_{12}+S'_{12}+S_{34}+S'_{34}+S} + \\ &(-1)^{S_{34}+S'_{34}+S}]\Big[(15J + {}^{15}/_2 j)\begin{Bmatrix} S_{12} & S'_{12} & 1 \\ S'_{34} & S_{34} & S\end{Bmatrix}\times \\ &\begin{Bmatrix} S_{12} & S'_{12} & 1 \\ {}^3/_2 & {}^3/_2 & {}^3/_2\end{Bmatrix}\begin{Bmatrix} S_{34} & S'_{34} & 1 \\ {}^3/_2 & {}^3/_2 & {}^3/_2\end{Bmatrix} - 30j\begin{Bmatrix} S_{12} & S'_{12} & 2 \\ S'_{34} & S_{34} & S\end{Bmatrix}\times \\ &\begin{Bmatrix} S_{12} & S'_{12} & 2 \\ {}^3/_2 & {}^3/_2 & {}^3/_2\end{Bmatrix}\begin{Bmatrix} S_{34} & S'_{34} & 2 \\ {}^3/_2 & {}^3/_2 & {}^3/_2\end{Bmatrix}\Big] \end{aligned} \quad (4)$$

The matrix elements are independent of M.[12] Table I lists

Table I. Nonvanishing Matrix Elements of the Operator (3) in the Basis (2)[a]

$\langle S_{12}S_{34}S\|$	$\|S'_{12}S'_{34}S\rangle$	J	j	J'	j'	J''	j''
000	000	0.0	0.0	−3.75	−9.375	−3.75	−9.375
110	110	−2.00	−10.600	−2.75	−2.875	−2.75	−2.875
220	220	−6.00	−3.000	−0.75	4.125	−0.75	4.125
330	330	−12.00	−20.400	2.25	−0.375	2.25	−0.375
011	011	0.0	0.0	−3.75	−9.375	−2.75	−2.875
101	101	0.0	0.0	−2.75	−2.875	−3.75	−9.375
111	111	−1.00	4.300	−2.75	−2.875	−2.75	−2.875
121	121	−3.00	−1.500	−2.75	−2.875	−0.75	4.125
211	211	−3.00	−1.500	−0.75	4.125	−2.75	−2.875
221	221	−5.00	−2.500	−0.75	4.125	−0.75	4.125
231	231	−8.00	−4.000	−0.75	4.125	2.25	−0.375
321	321	−8.00	−4.000	2.25	−0.375	−0.75	4.125
331	331	−11.00	−16.300	2.25	−0.375	2.25	−0.375
022	022	0.0	0.0	−3.75	−9.375	−0.75	4.125
112	112	1.00	−0.460	−2.75	−2.875	−2.75	−2.875
122	122	−1.00	−0.500	−2.75	−2.875	−0.75	4.125
132	132	−4.00	3.760	−2.75	−2.875	2.25	−0.375
202	202	0.0	0.0	−0.75	4.125	−3.75	−9.375
212	212	−1.00	−0.500	−0.75	4.125	−2.75	−2.875
222	222	−3.00	−1.500	−0.75	4.125	−0.75	4.125
232	232	−6.00	−3.000	−0.75	4.125	2.25	−0.375
312	312	−4.00	3.760	2.25	−0.375	−2.75	−2.875
322	322	−6.00	−3.000	2.25	−0.375	−0.75	4.125
332	332	−9.00	−9.060	2.25	−0.375	2.25	−0.375
033	033	0.0	0.0	−3.75	−9.375	2.25	−0.375
123	123	2.00	1.00	−2.75	−2.875	−0.75	4.125
133	133	−1.00	−7.70	−2.75	−2.875	2.25	−0.375
213	213	2.00	1.00	−0.75	4.125	−2.75	−2.875
223	223	0.0	0.0	−0.75	4.125	−0.75	4.125
233	233	−3.00	−1.500	−0.75	4.125	2.25	−0.375
303	303	0.0	0.0	2.25	−0.375	−3.75	−9.375
313	313	−1.00	−7.700	2.25	−0.375	−2.75	−2.875
323	323	−3.00	−1.500	2.25	−0.375	−0.75	4.125
333	333	−6.00	−0.600	2.25	−0.375	2.25	−0.375
134	134	3.00	3.900	−2.75	−2.875	2.25	−0.375
224	224	4.00	2.000	−0.75	4.125	−0.75	4.125
234	234	1.00	0.500	−0.75	4.125	2.25	−0.375
314	314	3.00	3.900	2.25	−0.375	−2.75	−2.875
324	324	1.00	0.500	2.25	−0.375	−0.75	4.125
334	334	−2.00	6.200	2.25	−0.375	2.25	−0.375
235	235	6.00	3.000	−0.75	4.125	2.25	−0.375
325	325	6.00	3.000	2.25	−0.375	−0.75	4.125
335	335	3.00	7.500	2.25	−0.375	2.25	−0.375
336	336	9.00	−1.500	2.25	−0.375	2.25	−0.375
000	220	0.0	−13.416	0.0	0.0	0.0	0.0
110	330	0.0	−5.499	0.0	0.0	0.0	0.0
011	211	0.0	7.589	0.0	0.0	0.0	0.0
011	231	0.0	−7.099	0.0	0.0	0.0	0.0
101	121	0.0	7.589	0.0	0.0	0.0	0.0
101	321	0.0	−7.099	0.0	0.0	0.0	0.0
111	331	0.0	−4.490	0.0	0.0	0.0	0.0
022	202	0.0	−6.000	0.0	0.0	0.0	0.0
112	132	0.0	5.387	0.0	0.0	0.0	0.0
112	312	0.0	5.387	0.0	0.0	0.0	0.0
112	332	0.0	−2.694	0.0	0.0	0.0	0.0
132	312	0.0	−0.240	0.0	0.0	0.0	0.0
132	332	0.0	−2.880	0.0	0.0	0.0	0.0
312	332	0.0	−2.880	0.0	0.0	0.0	0.0
033	213	0.0	−4.648	0.0	0.0	0.0	0.0
033	233	0.0	−9.295	0.0	0.0	0.0	0.0
123	303	0.0	−4.648	0.0	0.0	0.0	0.0
133	313	0.0	−1.200	0.0	0.0	0.0	0.0
133	333	0.0	−5.091	0.0	0.0	0.0	0.0
303	323	0.0	−9.295	0.0	0.0	0.0	0.0
313	333	0.0	−5.091	0.0	0.0	0.0	0.0
134	314	0.0	−3.600	0.0	0.0	0.0	0.0
134	334	0.0	−5.628	0.0	0.0	0.0	0.0
314	334	0.0	−5.628	0.0	0.0	0.0	0.0

[a] Elements are independent of M. $\langle S_{12}S_{34}S|\hat{H}_{ex}|S'_{12}S'_{34}S\rangle = \langle S'_{12}S'_{34}S|\hat{H}_{ex}|S_{12}S_{34}S\rangle$.

all the nonvanishing elements. Off-diagonal elements are found to depend only on j. Since biquadratic exchange parameters are usually 2 orders of magnitude smaller than the corresponding bilinear parameters, off-diagonal elements may to a good approximation be neglected.

An a posteriori justification of this procedure is obtained by calculating the contamination of wave functions due to off-diagonal elements with the final parameters (Table II) of this investigation. For the two lowest levels of the ground-state multiplet we calculate

$$\psi_2 = 0.9999|231\rangle - 0.0170|011\rangle - 0.0002|211\rangle$$

$$\psi_1 = 0.9999|330\rangle - 0.0135|110\rangle \quad (5)$$

Neutron Inelastic Scattering

Neutron inelastic scattering allows the direct measurement of spectroscopic transitions between the exchange split levels of the ground state. Selection rules and relative intensities for transitions $|S_{12}S_{34}S\rangle \rightarrow |S'_{12}S'_{34}S'\rangle$ can be derived from the differential neutron scattering cross section.

$$\frac{d^2\sigma}{d\Omega d\omega} = \frac{N}{Z}\left(\frac{\gamma e^2}{m_e c^2}\right)^2 \frac{k_1}{k_0} F^2(\vec{Q}) \exp\{-2W\} \exp\{-E(S_{12}S_{34}S)/kT\} \times \sum_{\alpha,\beta}\left(\delta_{\alpha\beta} - \frac{Q_\alpha Q_\beta}{Q^2}\right)\sum_{i,j} \exp\{i\vec{Q}\cdot(\vec{R}_i - \vec{R}_j)\} \times \sum_{M,M'} \langle S_{12}S_{34}SM|\hat{S}_i^\alpha|S'_{12}S'_{34}S'M'\rangle \times \langle S'_{12}S'_{34}S'M'|\hat{S}_j^\beta|S_{12}S_{34}SM\rangle \delta\{\hbar\omega + E(S_{12}S_{34}S) - E(S'_{12}S'_{34}S')\} \quad (6)$$

In eq 6 k_0 and k_1 are the wavenumbers of incoming and scattered neutrons, respectively, $\vec{Q}$ is the scattering vector, $F(\vec{Q})$ is the magnetic form factor, $\exp\{-2W\}$ is the Debye–Waller factor, and $\vec{R}_i$ is the space vector of the ith Cr^{3+} ion and α and β stand for x, y, z. The remaining symbols have their usual meaning. Formula 6 derives from the general cross-section formula for magnetic neutron scattering.[13]

Operators of the type $\hat{S}_i^\alpha$ in eq 6 are one-ion operators, and the corresponding matrix elements are best evaluated by using tensor operator techniques.[12] The procedure has been outlined for the case of a Cr^{3+} dimer.[9] The same principles can be used here. Finally, account has to be taken of the fact that our experiments were performed on a powdered sample, i.e., random orientation of the tetranuclear complexes with respect to $\vec{k}_0$ and $\vec{k}_1$. This means that the cross-section formula has to be averaged in $\vec{Q}$ space. For the $\vec{Q}$-averaged cross section of a transition $|S_{12}S_{34}S\rangle \rightarrow |S'_{12}S'_{34}S'\rangle$ we get expression 7[14]

$$\left\langle \frac{d^2\sigma}{d\Omega d\omega} \right\rangle_{\vec{Q}} = 20KF^2(Q) \frac{\exp\{-E(S_{12}S_{34}S)/kT\}}{Z} \times (2S+1)(2S'+1)\delta\{\hbar\omega + E(S_{12}S_{34}S) - E(S'_{12}S'_{34}S')\} \times \left(\delta(S_{12}S'_{12})(2S_{34}+1)(2S'_{34}+1)\begin{Bmatrix} S' & S & 1 \\ S_{34} & S'_{34} & S_{12} \end{Bmatrix}^2 \times \begin{Bmatrix} S_{34} & S'_{34} & 1 \\ 3/2 & 3/2 & 3/2 \end{Bmatrix}^2 \left[1 + (-1)^{S_{34}+S'_{34}} \frac{\sin(R_{34}Q)}{R_{34}Q}\right] + \delta(S_{34}S'_{34})(2S_{12}+1)(2S'_{12}+1)\begin{Bmatrix} S' & S & 1 \\ S_{12} & S'_{12} & S_{34} \end{Bmatrix}^2 \times \begin{Bmatrix} S_{12} & S'_{12} & 1 \\ 3/2 & 3/2 & 3/2 \end{Bmatrix}^2 \left[1 + (-1)^{S_{12}+S'_{12}} \frac{\sin(R_{12}Q)}{R_{12}Q}\right] + 4\delta(S_{12}S'_{12})\delta(S_{34}S'_{34})(-1)^{S+S'+S_{12}+S_{34}}(2S_{12}+1)(2S_{34}+1) \times \begin{Bmatrix} S & S' & 1 \\ S_{12} & S_{12} & S_{34} \end{Bmatrix}\begin{Bmatrix} S & S' & 1 \\ S_{34} & S_{34} & S_{12} \end{Bmatrix}\begin{Bmatrix} S_{12} & S_{12} & 1 \\ 3/2 & 3/2 & 3/2 \end{Bmatrix} \times \begin{Bmatrix} S_{34} & S_{34} & 1 \\ 3/2 & 3/2 & 3/2 \end{Bmatrix}\left[\frac{\sin(R_{13}Q)}{R_{13}Q}\right]\Bigg) \quad (7)$$

where $K = N(\gamma e^2/m_e c^2)^2(k_1/k_0)\exp\{-2W\}$ and $R_{ij} = |\vec{R}_i - \vec{R}_j|$. The following selection rules are obtained by inspection:

$$\Delta S = 0, \pm 1 \quad (8a)$$

$$\Delta S_{12} = 0 \quad \text{and} \quad \Delta S_{34} = 0, \pm 1 \quad (8b)$$

$$\Delta S_{12} = 0, \pm 1 \quad \text{and} \quad \Delta S_{34} = 0 \quad (8c)$$

In addition there is the general selection rule[9]

$$\Delta M = 0, \pm 1 \quad (9)$$

Table II. Exchange Parameters (cm^{-1}) for Deuterated Rhodoso Chloride As Obtained from an Analysis of the Neutron Inelastic Scattering Data[a]

J	J'	J''	j	j'
17.4 ± 1.1	22.7 ± 2.5	0 ± 3	−0.14 ± 0.36	0.90 ± 0.24

[a] j'' was set to zero.

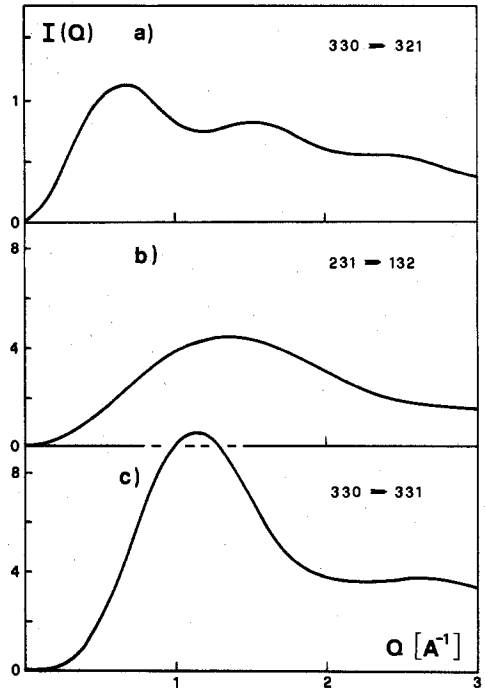

Figure 2. Q dependence of inelastic neutron scattering intensity of three selected transitions: (a) corresponding to the first interference term in (7), (b) corresponding to the second interference term in (7), (c) corresponding to the sum of the three interference terms in (7). The connection between $I(Q)$ and the Q averaged differential neutron scattering cross section of (7) is the following: $I(Q) = Z/K \times \exp\{-E(S_{12}S_{34}S)/kT\}\langle d^2\sigma/d\Omega d\omega\rangle_{\vec{Q}}$.

Formula 7 provides some very important information on the Q dependence of the scattering intensity. Since Q is an experimental variable, the observed Q dependence of intensity of a transition can be used in addition to its energy to make spectroscopic assignments. The three expressions in brackets in eq 7 are so-called interference terms reflecting the various separations of the Cr^{3+} ions in the tetranuclear complex.[15] The Q dependence of the scattering intensity of a given transition is

$$I(Q) \propto F^2(Q)[\text{combination of interference terms}] \quad (10)$$

In Figure 2 $I(Q)$ is plotted for three selected transitions.

Results and Analysis

Figure 3 shows a survey single-crystal absorption spectrum of deuterated rhodoso chloride. Part of the low-intensity structure near 15 000 cm^{-1} is enlarged in Figure 4. The figures serve to illustrate the effects of exchange coupling in the tetranuclear complex. The absorption bands in the 14 000–16 000-cm^{-1} region can be assigned to single excitations to ^2E and $^2T_1$. Due to the presence of two inequivalent chromium(III) centers in the molecule this part of the spectrum corresponds at least to a good approximation to a superposition of two Cr^{3+} spectra. The exchange splitting of the electronic ground state of the tetranuclear complex leads to the temperature dependences observed in Figure 4. The absorption near 30 000 cm^{-1} is due to double excitations to ^2E and $^2T_1$. They occur at approximately twice the energy of the corresponding single excitations. Both singly and doubly excited

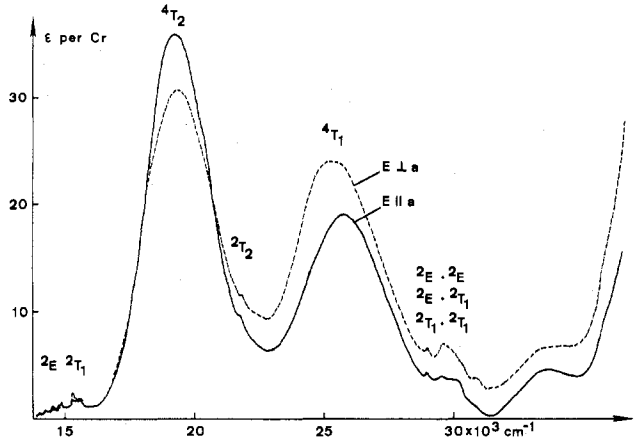

Figure 3. Polarized 6 K absorption spectrum of a single crystal of deuterated rhodoso chloride. Estimated crystal thickness was 0.1 mm. The spectrum was measured with the light propagating perpendicular to the well-developed *ac* face.

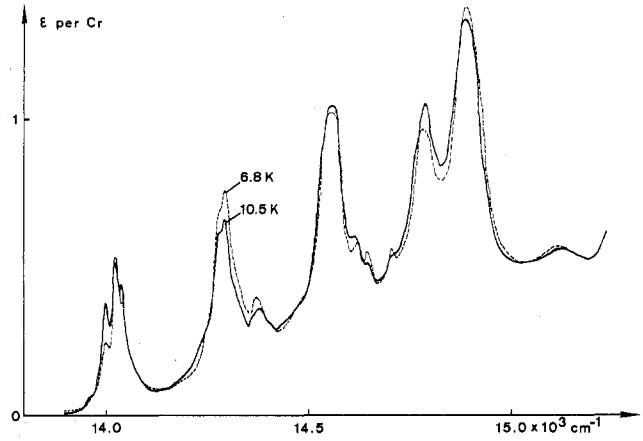

Figure 4. Low-energy part of a polarized single-crystal absorption spectrum. The light propagation was perpendicular to the *ac* face with the electric vector parallel to *a*.

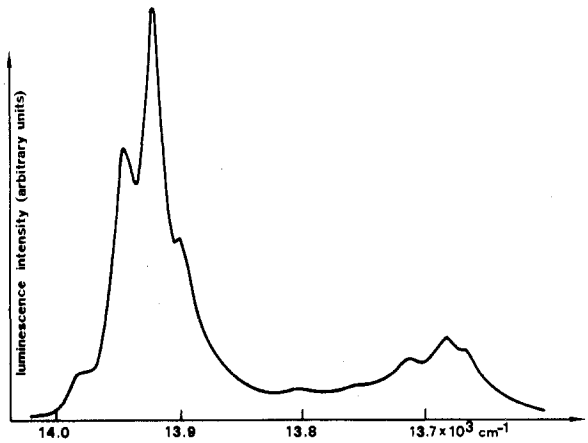

Figure 5. A 7 K luminescence spectrum of polycrystalline deuterated rhodoso chloride.

states are split by exchange interactions. This splitting is reflected in the structure of the absorption bands. The resolution, however, is rather poor, and a quantitative analysis of exchange effects in the excited states is not possible.

Luminescence occurs from the lowest excited state of the tetranuclear complex. It would be very interesting to know whether in this state the excitation is predominantly localized on Cr_1 and Cr_2 or alternatively on Cr_3 and Cr_4. We are not in a position to answer this question yet. However, the powder

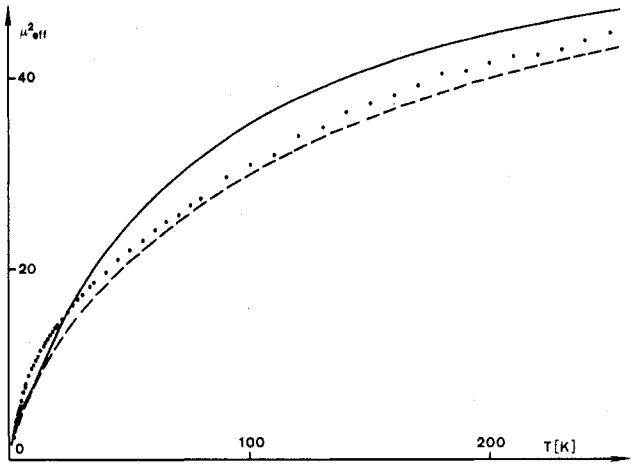

Figure 6. Magnetic susceptibility of deuterated rhodoso chloride (●). The full curve shows the result of a least-squares fit, in which g was set to 1.98, the two dominant parameters J and J' were refined, and all the other exchange parameters were set to zero. The broken curve is calculated (using g = 1.98) from the exchange parameters determined from neutron scattering (Table II).

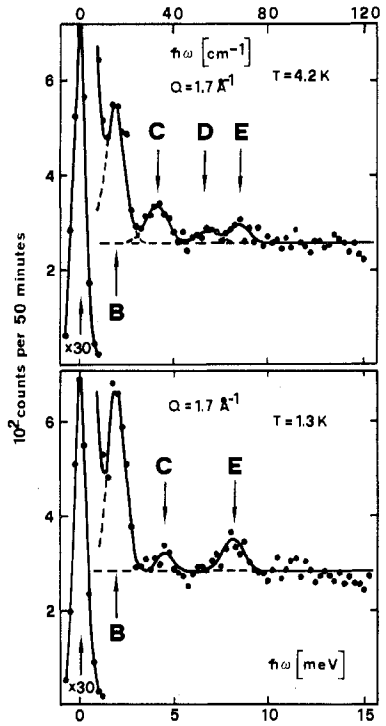

Figure 7. Triple-axis neutron inelastic scattering spectra of deuterated rhodoso chloride. The intense band at zero energy transfer is due to elastic and quasi-elastic scattering. The full curves represent least-squares fits to the experimental data assuming a linear background and approximating the peaks by Gaussians.

luminescence spectrum in Figure 5 demonstrates two points rather nicely: (i) energy transfer among the Cr^{3+} centers is so fast and efficient that luminescence is only observed from the lowest state of the tetramer; (ii) the transitions from the lowest excited state to the exchange split ground state are governed by rather strict selection rules. The zero phonon region of the luminescence is dominated by three bands, while the ground state is split into 44 levels.

We now turn to a detailed analysis of the exchange splittings in the electronic ground state. Figure 6 shows a plot of the magnetic susceptibility data. The sharp drop of μ_{eff}^2 below 10 K, which is also observed in the undeuterated compound, can only be understood if the lowest level of the exchange split

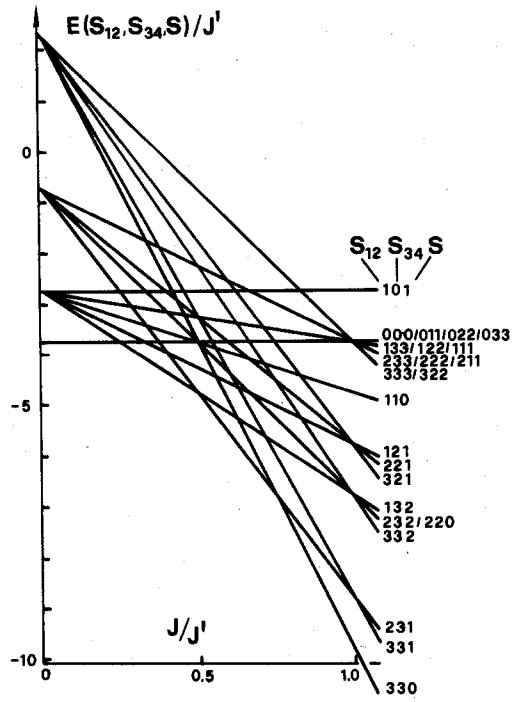

Figure 8. Part of a spin-level correlation diagram for the tetranuclear rhodoso ion. All interactions except J and J' are neglected.

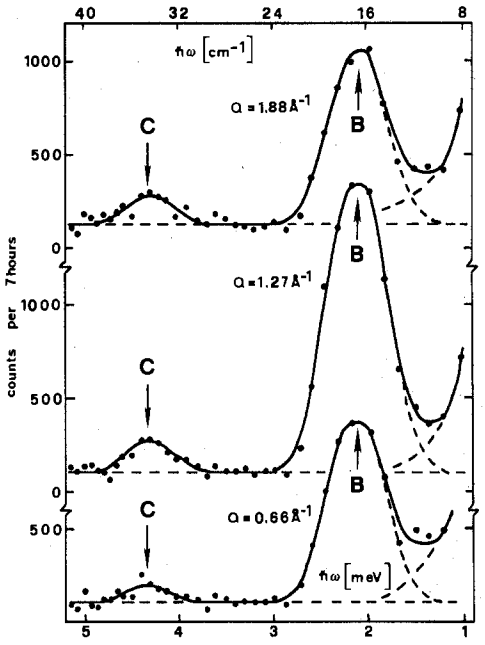

Figure 9. MARC neutron inelastic scattering spectra of deuterated rhodoso chloride at 1.3 K. The Q values refer to an energy transfer of 17 cm^{-1} (peak B). The curves were obtained as in Figure 7.

electronic ground state is a spin singlet. On the other hand it already indicates the presence of a close-lying triplet. Neutron inelastic scattering triple-axis spectra (Figure 7) confirm this. The temperature dependence of the spectra between 1.3 and 4.2 K reflects a change in Boltzmann populations. We thus conclude that there are at least two levels separated by not more than 4 cm^{-1}. If we assume J and J' to be the dominant terms in the exchange coupling, the ratio of J/J' is now fixed to a value close to 0.75 by inspection of Figure 8. We can therefore safely exclude the proposition made by Iwashita et al.[5] for the related Pfeiffer ion that J' is very strongly ferromagnetic. We are obviously close to the crossover region $|330\rangle/|231\rangle$.

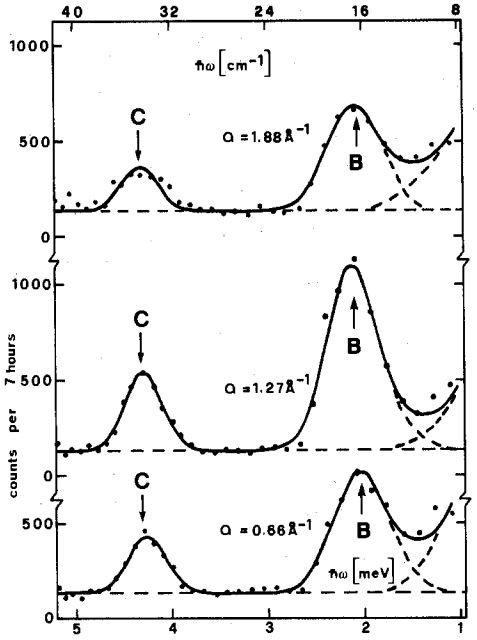

Figure 10. As in Figure 9, but at 4.2 K.

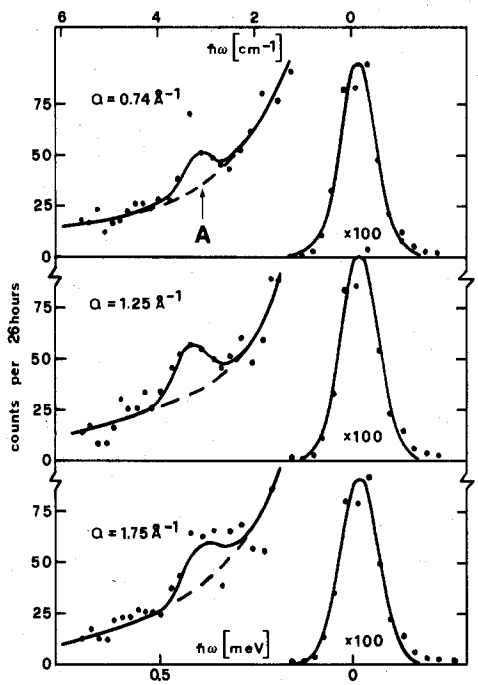

Figure 11. High-resolution MARC spectra at small energy transfer. The Q values refer to peak A. The curves were obtained as in Figure 7.

Next we try to refine the picture by a more complete analysis of our data and by extending our neutron scattering experiments. Figures 9 and 10 show two sets of MARC spectra at 1.3 and 4.2 K. Within the sets we recognize the Q dependence of the intensities. In Figure 11 we see the result of an experiment in which the tail of the elastic scattering peak is investigated under high resolution. The $|330\rangle \rightarrow |231\rangle$ transition can just be resolved.

Having made the obvious assignment of band A to the transition $|330\rangle \rightarrow |231\rangle$ we see immediately that the simplified picture of Figure 8 is not appropriate. According to this diagram we expect a peak at about 25 cm^{-1} corresponding to the rather intense transition $|231\rangle \rightarrow |132\rangle$. No peak is observed in this spectral range. This problem cannot be resolved by allowing J'' to take a nonzero value, because both

Table III. Observed and Calculated Neutron Inelastic Scattering Transition Energies and Intensities[a]

peak	T	Q	E_{obsd}, cm^{-1}	I_{obsd}	assign	E_{calcd}	I_{calcd}
A	4.2	0.74	3.1 ± 0.5	0.69 ± 0.11			0.62
A	4.2	1.25	3.2 ± 0.2	1.0 ± 0.09	|330⟩ → |231⟩	3.25	1.0
A	4.2	1.75	3.0 ± 0.6	0.83 ± 0.16			0.87
B	1.3	0.66	17.0 ± 0.6	0.61 ± 0.08			0.47
B	1.3	1.27	16.9 ± 0.3	1.00 ± 0.05			1.00
B	1.3	1.88	16.8 ± 0.6	0.56 ± 0.08	|330⟩ → |331⟩	16.83	0.46
B	1.3	1.70	15.3 ± 1.6	1.00 ± 0.1	|231⟩ → |132⟩	16.82	1.00
B	4.2	0.66	16.7 ± 0.6	0.35 ± 0.08	|231⟩ → |331⟩	13.58	0.28
B	4.2	1.27	17.0 ± 0.6	0.61 ± 0.06	unresolved		0.66
B	4.2	1.88	16.5 ± 0.6	0.41 ± 0.08			0.35
B	4.2	1.70	15.3 ± 1.6	0.73 ± 0.10			0.73
C	1.3	0.83	34.7 ± 1.6	0.04 ± 0.02			0.08
C	1.3	1.37	34.7 ± 0.8	0.08 ± 0.02			0.08
C	1.3	1.93	34.7 ± 1.6	0.07 ± 0.02	|231⟩ → |232⟩	34.66	0.04
C	1.3	1.70	33.1 ± 2.4	0.09 ± 0.04	|231⟩ → |220⟩	34.66	0.10
C	4.2	0.83	34.6 ± 0.8	0.20 ± 0.03	unresolved		0.22
C	4.2	1.37	34.6 ± 0.7	0.25 ± 0.03			0.24
C	4.2	1.93	34.5 ± 0.8	0.14 ± 0.03			0.12
C	4.2	1.70	36.3 ± 4.0	0.25 ± 0.05			0.27
D	4.2	1.70	53.8 ± 4.8	0.07 ± 0.03	|231⟩ → |332⟩	47.36	
					|231⟩ → |221⟩	51.99	0.09
					unresolved		
E	1.3	1.70	66.2 ± 3.2	0.20 ± 0.06			0.14
E	4.2	1.70	68.6 ± 4.0	0.12 ± 0.05	|330⟩ → |321⟩	67.30	0.07

[a] Intensities were calculated by using formula 7. The intensity of the most intense transitions of both triple axis and MARC spectra was set equal to 1. The calculated energies were obtained from the parameters in Table II.

|231⟩ and |132⟩ are shifted by the same amount. We are therefore forced to introduce biquadratic terms in the exchange Hamiltonian, in order to shift the above transition to an energy where inelastic scattering is observed.

Table III lists energies, intensities, T dependencies, and Q dependencies of the five observed peaks A–E. From a complete analysis of these data it is possible to make definite spectroscopic assignments. The results of the analysis are also given in Table III. As one can see some of the peaks are composed of two or three unresolved transitions. It is therefore very important to use the transition intensities and Q dependences in addition to their energies in order to make assignments. This agreement between observed and calculated quantities is good. The results are summarized in Figure 12 and Table II.

As an additional test for the exchange parameters we calculated μ_{eff}^2 by using the formula[11]

$$\mu_{eff}^2 = g^2 \frac{\sum_{S_{12}S_{34}S} S(S+1)(2S+1)\exp\{-E(S_{12}S_{34}S)/kT\}}{\sum_{S_{12}S_{34}S} (2S+1)\exp\{-E(S_{12}S_{34}S)/kT\}} \quad (11)$$

The conditions under which eq 11 is applicable have been discussed by Griffith.[11] Even though first-order Zeeman splittings are of the same order of magnitude as kT at very low temperatures, we obtained only very small differences by using eq 11 and a more general formula.[16] The result is shown in Figure 6. The agreement with the experimental data is satisfactory. The rather large standard deviations of the exchange parameters are mainly responsible for the fact that the fit is not quantitative. In addition a possible temperature dependence of exchange will produce deviations at high temperatures.

For comparison we made a number of least-squares fits to the susceptibility. Between two and five parameters were simultaneously refined. Refining J and J' only, with the other parameters set to zero and $g = 1.98$, we obtained a unique solution: $J = 12.3 \pm 0.4$ cm^{-1}, $J' = 15.7 \pm 0.6$ cm^{-1}. The fit is rather poor (Figure 6), and the standard deviations obtained for the parameters are meaningless. As expected an increase of the number of adjustable parameters markedly improved

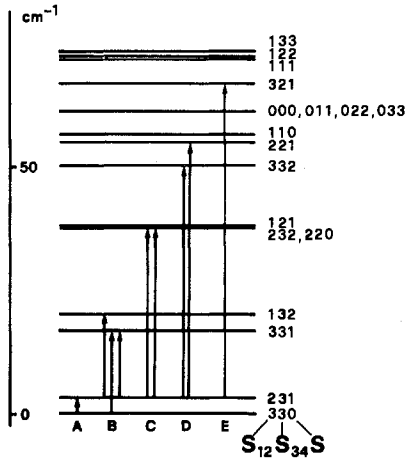

Figure 12. Energy splittings of the lowest levels of the electronic ground state (parameters Table II) and observed inelastic neutron scattering transitions.

the fits. However, the results obtained cannot be considered to be physically meaningful. Nonunique solutions were obtained, and it could be shown that excellent agreement with the susceptibility curve could be obtained by physically absurd choices of the five parameters J, J', J'', j, and j'. Clearly there is not enough structure in the susceptibility curve to warrant the simultaneous refinement of five parameters. Magnetic susceptibility measurements are of great value to determine orders of magnitude of the major exchange parameters in a coupled complex and to establish trends in a series of related compounds. When the number of parameters is as large as in our complex, however, the limitations of the technique become obvious.

Discussion

The observed exchange splitting pattern in the ground state of deuterated rhodoso chloride can well be described by a Hamiltonian of type (3) containing bilinear and biquadratic interaction terms. Although contributions from three- and four-body interaction terms are expected to be of the same order of magnitude as the biquadratic contributions,[17] the

accuracy of our experimental data does not allow an estimate of their importance. Potentially, neutron inelastic scattering is a method which should allow us to carry the analysis further. There are more than 200 allowed transitions within the exchange-split ground-state manifold. If a sufficiently large number of them could be individually resolved, we should be in position to really test the applicability of the operator (3). So far we have mainly been limited by a lack of resolution, a limitation which is not inherent in the method itself but which has to do with our particular experimental conditions. We are planning to extend our measurements, particularly to improve the resolution.

That J and J' are the dominating terms in the exchange interaction of the rhodoso complex is no surprise. It corresponds both to what we expect intuitively and to the conclusions arrived at by Flood et al. about the structurally related Pfeiffer complex: $J = 14.6\ cm^{-1}$, $J' = 27.82\ cm^{-1}$.[4] But even if the parameters J and J' for the two complexes are similar, the ordering of the levels in the ground state may be quite different. The reason for this is obvious from Figure 8; a small change of the J/J' ratio has a big effect on the level ordering. From the magnetochemical evidence produced for Pfeiffer azide,[4,5] the lowest level in the ground-state multiplet is a spin triplet and not a spin singlet as in rhodoso chloride.

From a comparison with mono- and dihydroxo-bridged dinuclear chromium(III) complexes, an antiferromagnetic sign is expected for J, even though the Cr–O–Cr angle of the monohydroxo bridge is rather small 133°.[18] The same is not necessarily true for J'. The following distances and angles were determined for this double bridge:[2] Cr–O, 1.96 (3) Å; Cr–Cr, 2.91 (1) Å; Cr–O–Cr, 96°. The Cr–O distance is comparable to the corresponding distances in dimeric complexes.[18] However, both Cr–Cr and Cr–O–Cr are smaller than in any dinuclear chromium(III) complex.[19] Finding ferromagnetic contributions to dominate antiferromagnetic ones thus leading to a negative J' would therefore be little surprise to most magnetochemists. Instead J' is found to be antiferromagnetic and larger than J.

A brief comment can be made about the biquadratic exchange parameters determined in this study. Both j and j' could not be determined very accurately. But still there is little doubt that j is close to zero, while j' is of the order of a few percent of the corresponding bilinear term J'. According to Andersons theory[20] j is expected to be of the order of 1% of J for true biquadratic exchange. Large biquadratic parameters are usually interpreted in terms of exchange striction.[21] There are several examples of dioxo- and dihydroxo-bridged dinuclear Cr^{3+} species in which large biquadratic exchange parameters were found.[22,23]

Acknowledgment. We thank K. Mattenberger and O. Vogt of the Laboratorium für Festkörperphysik, ETH, for performing the magnetic susceptibility measurements. This work was supported by the Swiss National Science Foundation (Grant No. 2.420-0.75).

Registry No. $[Cr_4(OH)_6(NH_3)_{12}]Cl_6 \cdot 4H_2O$, 22533-71-7; $[Cr_4(OD)_6(ND_3)_{12}]Cl_6 \cdot 4D_2O$, 70891-73-5.

References and Notes

(1) S. M. Jørgensen, *J. Prakt. Chem.*, **30**, 1 (1884); **45**, 45 (1892).
(2) E. Bang, *Acta Chem. Scand.*, **22**, 2671 (1968).
(3) M. T. Flood, R. E. Marsh, and H. B. Gray, *J. Am. Chem. Soc.*, **91**, 193 (1969).
(4) M. T. Flood, C. G. Barraclough, and H. B. Gray, *Inorg. Chem.*, **8**, 1855 (1969).
(5) T. Iwashita, T. Idogaki, and N. Uryû, *J. Phys. Soc. Jpn.*, **30**, 1587 (1971).
(6) M. Sorai and S. Seki, *J. Phys. Soc. Jpn.*, **32**, 382 (1972).
(7) M. Drillon, J. Darriet, P. Delhaes, G. Fillion, R. Georges, and P. Hagenmüller, *Nouv. J. Chim.*, **2**, 475 (1978); M. Drillon, J. Darriet, and R. Georges, *J. Phys. Chem. Solids*, **38**, 411 (1977).
(8) J. R. Rebouillat, thèse de docteur, CNRS, Grenoble, 1972.
(9) H. U. Güdel and A. Furrer, *Mol. Phys.*, **33**, 1335 (1977).
(10) H. U. Güdel, A. Stebler, and A. Furrer, *Inorg. Chem.*, **18**, 1021 (1979).
(11) J. S. Griffith, *Struct. Bonding (Berlin)*, **10**, 87 (1972).
(12) U. Fano and G. Racah, "Irreducible Tensorial Sets", Academic Press, New York, 1959, p 84 ff.
(13) W. Marshall and S. W. Lovesey, "Theory of Thermal Neutron Scattering", Clarendon Press, Oxford, 1971, Chapter 5.
(14) Derivation of formula 7 is lengthy. Details will be described in U. Hauser, Ph.D. Thesis, University of Bern, 1979.
(15) A. Furrer and H. U. Güdel, *Phys. Rev. Lett.*, **39**, 657 (1977).
(16) J. H. van Vleck, "The Theory of Electric and Magnetic Susceptibilities", Oxford University Press, 1932, p 182.
(17) R. G. Munro and M. D. Girardeau, *J. Magn. Magn. Matter.*, **2**, 319 (1976).
(18) D. J. Hodgson, *Prog. Inorg. Chem.*, **19**, 173 (1975).
(19) R. P. Scaringe, W. E. Hatfield, and D. J. Hodgson, *Inorg. Chem.*, **16**, 1600 (1977).
(20) P. W. Andersen in "Solid State Physics", Vol. 14, F. Seitz and D. Turnbull, Eds., Academic Press, New York, 1963, p 99.
(21) K. N. Shrivastava, *Phys. Lett. A*, **56**, 399 (1976).
(22) H. van den Boow, A. J. J. van Dijsseldonk, and J. C. M. Henning, *J. Chem. Phys.*, **66**, 2368 (1977), and references therein.
(23) A. Beutler, H. U. Güdel, T. R. Snellgrove, G. Chapuis, and K. Schenk, *J. Chem. Soc., Dalton Trans.*, 983 (1979).